Core effects in lithium hydride

L. Bellaiche*
LURE, Bâtimet 209, Université Paris-Sud, 91405 Orsay Cedex, France
and Laboratoire de Physique des Solides associé au C.N.R.S., Université Pierre et Marie Curie,
Tour 13, Boîte Postale 79, 4 place Jussieu, 75252 Paris Cedex 05, France

K. Kunc
Laboratoire de Physique des Solides associé au C.N.R.S., Université Pierre et Marie Curie,
Tour 13, Boîte Postale 79, 4 place Jussieu, 75252 Paris Cedex 05, France
(Received 12 February 1996; revised manuscript received 4 November 1996)

Calculations of the directional Compton profiles and of the anisotropies of Compton scattering are reported, based on density-functional theory within the local-density approximation, performed using a plane-wave basis, and using (i) pseudopotentials and (ii) full, unscreened Coulomb potentials for both Li and H atoms. The pseudopotential calculations yield Compton profiles with unsatisfactory agreement with experiment. The reason of this failure is discussed. It is then shown that, with the total Coulomb potentials, converged results can be obtained, and that the Compton profiles obtained are in excellent agreement with experiment. Possibilities (and limits) of extending the plane-wave calculations with the full Coulomb potentials to other atoms and substances are discussed. Furthermore, a simple method is proposed that allows the reproduction of the full Coulomb potential results at a much lower cost, by orthogonalizing the pseudo-wave-functions to the core orbitals calculated separately. [S0163-1829(97)00708-X]

I. INTRODUCTION

Although the Compton effect has been known for more than 70 years, its importance for solid state physics has only been recognized since the beginning of the 1970's.[1,2] As a matter of fact, Compton scattering is a very straightforward way of probing the ground-state electronic structure of materials and, during the past two decades, a large volume of experimental data has been accumulated, concerning mainly light atoms and their compounds (for a review, see, e.g., Refs. 1,3), as a consequence of the development of tunable high-flux x-ray sources. From our point of view, Compton scattering offers an excellent possibility of verifying the calculations of electronic structure. Being a ground-state property, the Compton effect is amenable to treatment by the density-functional (DF) theory and, within the framework of the local-density approximation (LDA), it allows one to judge the approximations involved or the assumptions made. It turns out that Compton profiles are fairly sensitive to details of the electronic valence-charge distribution.

A few theoretical works which proceed along similar lines as our present work deserve to be mentioned: The pseudopotential calculations of Compton profiles in beryllium,[4] the Hartree-Fock calculations on LiH and BN,[5,6] the works on graphite and intercalation compounds,[7–9] still another pseudopotential calculation on BN,[10] and finally our previous work on LiH within the Hartree-Fock theory and in the basis of Wannier-type functions.[11] A more extensive review can be found, e.g., in Ref. 3.

In this paper we report calculations, in a plane-wave basis, of the directional Compton profiles and their anisotropies which are based on using (besides the DF theory and the LDA) the norm-conserving pseudopotentials but also the full, unscreened Coulomb potentials for *both* Li and H atoms. We show that employing pseudopotentials does not succeed in reproducing accurately the Compton profiles. On the other hand, when avoiding the pseudization of the valence wave function by using the full, unscreened Coulomb potentials, the theoretical Compton profiles become in excellent agreement with experiment. In this study, we identify the problem of the pseudopotential method in the description of the Compton profiles and propose a simple method based on the orthogonalization of the valence pseudo-wave-functions to the lithium core orbital, which allows us to reproduce, within the framework of pseudopotential calculations, the Compton results obtained with the full Coulomb potentials. Finally, the possibilities, as well as the limits, of extending the plane-wave calculations with the full Coulomb potentials to other atoms and substances are discussed.

We start by describing in Sec. II the different methods we will use in this article, then discuss in Sec. III the results of the pseudopotentials calculations, and the convergence of the all-electron calculations for the basic ground-state properties of LiH. Finally, Sec. IV concerns the main aspect of this work, i.e., the advantages and limitations of the different electronic methods used to describe the Compton profile.

II. ELECTRONIC METHODS

A. Total-energy calculations: Pseudopotential and full nuclear potential

For the calculation of the total energy of the LiH crystal we first develop the one-electron wave functions $\psi_{n,\vec{k}}$ in a plane-wave basis:[12]

$$\psi_{n,\vec{k}}=\sum_{\vec{G}} C_{n,\vec{k}}(\vec{G})\exp[i(\vec{k}+\vec{G})\cdot\vec{r}], \tag{1}$$

where $\vec{k}$ is a wave vector restricted to the first Brillouin zone (BZ), n is the quantum number indexing the band, $\vec{G}$ stands for reciprocal-lattice vectors, and $C_{n,\vec{k}}(\vec{G})$ are the coefficients of the development.

Then we use the local-density approximation,[13] with the Ceperley-Alder exchange and correlation[14] as parametrized by Perdew and Zunger.[15] The $\vec{k}$-space summation is performed using ten ''special points'' which, in the Monkhorst-Pack notation,[16] correspond to $q_1q_2q_3=444$.

The unscreened $-1/r$ Coulomb potential is always used for hydrogen, while the lithium potential is described by two different techniques: (i) within the pseudopotential approach, where the pseudopotential of the lithium is generated by the Kerker method,[17] using the $1s^22s^1$ and $1s^22p^{0.25}3d^{0.25}$ atomic electronic configurations for obtaining the s-, p-, and d-components of the pseudopotential, while the correction[18] for the nonlinearity of the exchange and correlation of lithium is taken into account; (ii) using the all-electron description, where we give up to the frozen-core approximation for Li and deal with the full nuclear potential $-3/r$. In the all-electron approach, the system studied consists of the nuclei $+3e$ and $+1e$, and of four electrons per primitive cell; compared to the pseudopotential calculations, the core electrons are dealt with explicitly, on the same footing as the valence ones. The information that one obtains in this Coulomb potential calculation is the ''correct'' behavior of the valence wave function in the core regions of lithium (in particular, the existence of a node)—which will be used for assessing its importance for the Compton effect.

B. The orthogonalization method

We have also attempted to ''reconstruct'' the complete valence wave function from the results obtained in the pseudopotential calculation. The procedure we employ consists in orthogonalizing the pseudo-wave function with respect to the core wave function — so as to complete the information normally missed in the pseudopotential framework, but at a much less cost than by performing the full Coulomb potential calculations.

It is easy to demonstrate that two wave functions $\psi_{n_1,\vec{k}_1}$ and $\psi_{n_2,\vec{k}_2}$ belonging to two different bands n_1 and n_2 can be nonorthogonal only if the vectors $\vec{k}_1$ and $\vec{k}_2$ are identical. This implies that we have to orthogonalize the valence wave functions, obtained within the pseudopotential approach, with respect to the corresponding core ones separately for everyone of the $\vec{k}$ vectors needed.

Let us first pay attention to the core functions $\psi_{1,\vec{k}}$ (i.e., the ''first'' ones, which correspond to the lowest Kohn-Sham energies in an ''all-electron'' calculation). We start by expressing them in terms of localized orbitals:

$$\psi_{1,\vec{k}}(\vec{r})=\frac{1}{N_{\mathrm{BL}}}\sum_{\vec{R}_{\vec{n}}}\phi_{\mathrm{core}}(\vec{r}-\vec{R}_{\vec{n}})\exp[i\vec{k}\cdot\vec{R}_{\vec{n}}], \tag{2}$$

where $\vec{R}_{\vec{n}}$ runs over the Bravais lattice, having N_{BL} sites, $\phi_{\mathrm{core}}(\vec{r}-\vec{R}_{\vec{n}})$ is a localized orthogonal orbital centered on the site $\vec{R}_{\vec{n}}$. The easiest way of getting this localized orbital is to take it from an atomic calculation. By combining Eqs. (1) and (2), we find that the coefficients $C_{1,\vec{k}}(\vec{G})$ of the plane-wave expansion for $\psi_{1,\vec{k}}$ are proportional to the Fourier transform of the localized orbital:

$$C_{1,\vec{k}}(\vec{G})\propto\int\phi_{\mathrm{core}}(\vec{r})\exp[-i(\vec{k}+\vec{G})\vec{r}]d\vec{r}. \tag{3}$$

Once the core functions $\psi_{1,\vec{k}_i}$ are constructed within a plane-wave expansion [Eq. (1)] from the localized orbital [Eq. (3)], we apply, as already done in the Ref. 4, the Gramm-Schmidt orthogonalization, which becomes particularly simple when only two functions are dealt with:

$$\psi^{\mathrm{rec}}_{2,\vec{k}}=\alpha[\psi^{\mathrm{pseudo}}_{2,\vec{k}}-\psi_{1,\vec{k}}(\langle\psi_{1,\vec{k}}|\psi^{\mathrm{pseudo}}_{2,\vec{k}}\rangle)]. \tag{4}$$

Here $n=1,2$ stands for the core and the valence band, $\psi^{\mathrm{rec}}_{2,\vec{k}}$ is the reconstructed valence (Bloch) wave function, $\psi^{\mathrm{pseudo}}_{2,\vec{k}}$ is the valence function obtained within the pseudopotential approach, and $\psi_{1,\vec{k}}$ is the core Bloch wave function constructed as explained above; α is the normalization factor, and $\langle\psi_{1,\vec{k}}|\psi^{\mathrm{pseudo}}_{2,\vec{k}}\rangle$ denotes the scalar product of the core functions with the pseudopotential valence one.

TABLE I. The equilibrium properties of LiH crystal (lattice constant a_0, bulk modulus B_0 and pressure derivative B_0' of the bulk modulus) predicted by the present peudopotential calculations with ten special $\vec{k}$ points for BZ sampling and the kinetic energy cutoff of 100 Ry, compared with the experimental values. Results of other calculations are quoted as well. The zero-point vibrations are not accounted for.

	a_0 (Å)	B_0 (Mbar)	B_0'
Present work	4.11	0.34	3.01
Other work [a]	3.90	0.40	
Other work [b]	3.34	0.66	3.57
Other work [c]	4.10	0.34	
Other work [d]	4.11	0.35	2.96
Experiment	4.06 [e]	0.336–0.362 [f]	3.80 [g]

[a]See Ref. 20.
[b]See Ref. 21.
[c]See Ref. 5.
[d]See Ref. 11.
[e]See Ref. 35.
[f]See Ref. 36.
[g]See Ref. 37.

III. STATIC PROPERTIES

A. Pseudopotential results

The static equilibrium quantities predicted by the pseudopotential approach and shown in Table I are obtained by fitting by the Murnaghan equation[19] the energies calculated for seven different volumes; they correspond to the plane-wave cutoff of 100 Ry. At this kinetic energy, all static properties are safely converged; in fact, we have observed that the second decimal of the lattice constant a_0, expressed in Å, is stable starting from the cutoff of 50 Ry, and that the convergence of the bulk modulus B_0 occurs even earlier: the second decimal of B_0, expressed in Mbar, is stable starting from the cutoff of 36 Ry. On the other hand, the convergence

of B_0' (the pressure derivative of the bulk modulus) requires more numerical effort: the second decimal of B_0' only becomes stable at cutoffs $\geqslant 70$ Ry. Somewhat surprisingly for a LDA calculation, our results approximate the experimental value of a_0 from above.

In Table I, we also report theoretical predictions of four other works. Neither of the results quoted in Table I includes the effect of the zero-point lattice vibrations. One of these four studies is fairly similar to our present calculations: Martins[20] performed LDA calculations with the Ceperley-Alder correlation, and using a pseudopotential with a nonlinear core-correction for lithium and the unscreened Coulomb potential for hydrogen. His study differs from ours by a few technical points, essentially the atomic configurations to generate pseudopotentials, which demonstrates that the choice of the atomic configurations is by no means negligible: our present results disagree with the results of Ref. 20 by about 5% for a_0 to some 15% for B_0, and it could seem that our equilibrium values are closer to the experiment than in Ref. 20. However, since it has been estimated that accounting for the zero-point vibrations implies increasing the lattice constant of LiH by approximately 1.7–3.5 %,[20–22] some caution should be exercised in judging which of the calculations reported in Table I is actually the most realistic.

On the other hand, there is no doubt that the nonlinear core correction for lithium is essential in LiH: in the study of Rodriguez and Kunc,[21] neglecting this core correction led to the lattice constant far too small and to the bulk modulus too high—even when the zero-point vibrations were subsequently taken into account.

The last two theoretical results reported in Table I concern Hartree-Fock calculations. One[5] is a standard calculation, yielding optimized Bloch wave functions. The second[11] refers to an approach, which demonstrates that a large part of the optimization of the Hartree-Fock calculations can be avoided by transferring some local aspects of the Wannier-type orbitals from small systems to the crystal. We observe that the latter two calculations give essentially identical predictions for a_0 and B_0 and that, somewhat surprisingly, these results are quasi-identical with our present LDA calculations. As for the values of B_0', i.e., the third derivative of the total energy $E^{\rm tot}$ with respect to the volume V, they are too uncertain to be used for judging the quality of one or another calculation: the experiments are approximate and also the Murnaghan fit reveals a considerable statistical error [e.g., when including (or leaving out) one more (or one less) calculated point $E^{\rm tot}(V)$].

B. The convergence of the all-electron method in plane-wave basis

The first results suggesting that realistic converged plane-wave calculations with the unscreened Coulomb potential $-Z/r$ are feasible for LiH date back to 1988–89.[23] The LDA energies of solid hydrogen were determined, using the bare Coulomb potential in Ref. 24 [plane-wave cutoff $E^{\rm pw}=150$ Ry (Refs. 25)]. The possibility of extending such a treatment to heavier atoms was examined by Teter,[26] who calculated the equation of state of carbon in diamond structure, in plane-wave basis as well ($E^{\rm pw}=600$ Ry). Now we start by reexamining more closely the question of convergence of the all-electron calculations with the number of plane waves. In Table II we illustrate the effect of increasing the number of plane waves on static properties; the quantity $f_{\rm ce}$ quoted in this table is the ''convergence-error factor,'' which will be introduced and further discussed in Sec. V.

TABLE II. Convergence test for the static equilibrium in LiH (lattice constant a_0, bulk modulus B_0 and pressure derivative B_0' of the bulk modulus) calculated using the unscreened potentials $-3/r$ and $-1/r$. The quantity $f_{\rm ce}$ is the ''convergence-error factor'' defined by Eq. (13). The total energy was evaluated at seven lattice constants between $a=3.6$ Å and 4.2 Å and interpolated by the Murnaghan equation; ten special $\vec{k}$ points were used for BZ sampling, $E^{\rm pw}$ denotes the kinetic energy cutoff. The contribution of the zero-point vibrations was not taken into account.

$E^{\rm pw}$ (Ry)	a_0 (Å)	B_0 (Mbar)	B_0'	$f_{\rm ce}$
72	3.94	0.44	3.43	0.0050
100	3.95	0.40	1.57	0.0031
140	3.91	0.39	3.74	0.0017
180	3.92	0.40	2.87	0.0011
210	3.91	0.40	3.19	0.0009
240	3.91	0.40	3.48	0.0007
Experiment	4.06 [a]	0.336–0.362 [b]	3.80 [c]	

[a]See Ref. 35.
[b]See Ref. 36.
[c]See Ref. 37.

Judging from the values of a_0 and B_0, one obtains converged results with the kinetic energy cutoffs starting from 140 Ry. Here we do not take into account the behavior of the pressure derivative B_0', because the error margin of its calculations is rather large — a consequence of the statistical fluctuations in the Murnaghan fitting[19] — and the experimental value is approximate as well. Like in most density-functional calculations, the predicted lattice constant is now lower than the experimental one — in this respect, the pseudopotential calculations on LiH reported in Table I are atypical.

It is interesting to note that another ''all-electron'' calculation,[22] viz., one using the augmented plane-wave method, predicts a value of the lattice constant of 3.93 Å, when neglecting the zero-point vibrations. This value is indeed very close to the one we obtained when using the ''simplest'' plane waves for both core and valence states.

The lattice constant obtained with the full Coulomb potentials is 3.7% under the experimental value. The agreement somewhat improves when we account for the effect of the zero-point vibrations, which tend to increase the lattice parameter: when the estimate of 1.7–1.8 % (or 3.5%), for the influence of the zero-point energy, derived in Refs. 21,22 (Ref. 20), is used, the discrepancy decreases by half (or exactly cancels). As for the bulk modulus, the estimates for the effect of the zero-point motion vary between -32% and -22% (Refs. 21 and 20); whatever its exact magnitude, this effect moves our calculated B_0 towards the experiment (if not somewhat beyond).

On the other hand, if we neglect the effect of the zero-point vibrations, the prediction for the lattice constant obtained by the pseudopotential method (see Table I) turns out to be slightly better than in the calculations with the full

TABLE III. Convergence, within the full Coulomb potentials calculations, of the core radial density maximum $\max_{\text{core}}$ and of node_{val}, the position of the node of the valence wave function at the Γ point, calculated in the [100] direction, versus the kinetic energy cutoff E^{pw}. N^{pw} denotes the number of planes waves included in the calculations of the wave functions.

E^{pw} (Ry)	N^{pw}	$\max_{\text{core}}$ (a.u.)	node_{val} (a.u.)
72	1052	0.41	0.96
100	1723	0.38	0.96
140	1845	0.35	0.93
180	4149	0.34	0.92
210	5213	0.34	0.92
240	6366	0.34	0.92

Coulomb potentials, which employ one approximation *less*. Apparently, the pseudopotential calculations on LiH benefit from some sort of compensation between the LDA and the pseudopotential approximation.

The major difficulty, known and expected, with the full Coulomb potential calculations is in reaching convergence of the quantities that depend on the core electrons' wave functions. In order to verify how well the lithium core can be described in the plane-wave calculations, we report in Table III the convergence of two quantities directly related to the core size: the position, along the (100) direction, of the maximum of the core radial density — defined by $r^2 n_c$, where the core charge density n_c is obtained from the wave functions associated with the lowest eigenvalue — and the position, again along the (100) direction, of the node of the valence wave function at the Γ point. It is understood that the origin is on the lithium atom, and the lattice parameter used is the one minimizing energy in the calculations with 210 Ry.

We can see from Table III that the full convergence of the core-related quantities is reached for the kinetic energy cutoff of 180 Ry — which explains the analogous convergence properties of the lattice constant and bulk modulus observed in Table II. The above results show clearly that realistic plane-wave calculations using the bare Coulomb potentials are possible in solids — on the condition that the Fourier expansions are sufficiently ''long ranged'' (in the G space) to reproduce the small size (in the real space) of the core orbitals. Calculations at this scale are possible with supercomputers becoming a standard tool in physics, and even more so with the appearance of the iterative methods of the Car-Parrinello type. The relatively large size and the corresponding computer cost of these calculations are partly compensated by the overwhelming simplicity of dealing with the Coulomb potentials, as well as by the more pronounced effect of vectorization of the codes (local potentials). Solving the Schrödinger equation in a plane-wave basis is not the most appropriate way of dealing with the localized states, such as core orbitals. Nonetheless, this basis is by no means powerless when it comes to describing atomic states of a certain (i.e., not too small) spatial extent. It may also be useful to remember that, unlike most codes designed for the spherically symmetrical problem (atomic calculations), the plane-wave algorithms do not involve any spherical averaging of the Hartree potential. This may represent certain conceptual advantage, nevertheless, in practice, the finite size of the basis set imposes another constraint on the sphericity of the potentials involved, viz., their shape is approximated by polyhedra.

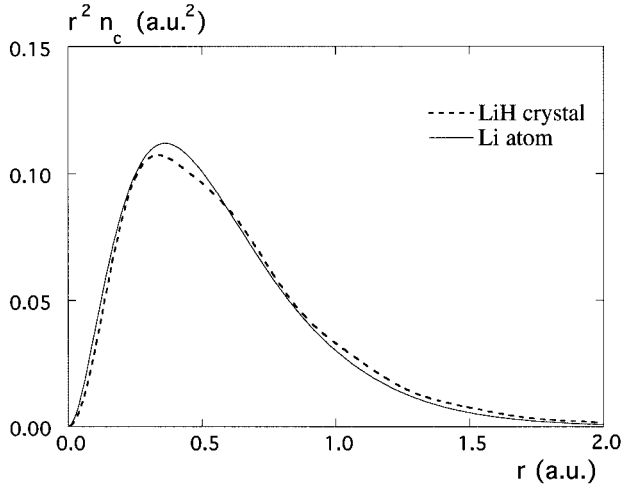

FIG. 1. Radial density of core electrons $r^2 n_c$ in the lithium atom (solid lines) and along the [100] direction in the LiH crystal (dotted lines), as calculated with the full Coulomb potentials using the cutoff of 210 Ry and the Ceperley-Alder correlation.

Taking as the simplest example a spherically symmetrical potential $V(r)$, it is obvious that, when represented by a finite plane-wave expansion, the potential becomes directionally dependent. The surfaces of constant potential $V(r)=E$ will be planes, as many different ones as there are independent directions $\vec{G}$ in the plane-wave expansion. As a result, every sphere will be approximated, more or less faithfully, by a polyhedron.

This finding is not a new problem; it is not a consequence of replacing the pseudopotentials by the unscreened Coulomb potentials, but an inherent property of the plane-wave basis set. The ''nonsmoothness'' does not usually have consequences in the pseudopotential calculations, but one may wonder whether this imperfect sphericity does not become critical when the spherical ''objects'' to represent are of much smaller size. The first check to perform is thus to examine how well (how smoothly) any given set of $\vec{G}$ vectors can approximate a sphere.

We have verified that the present full Coulomb potential calculations in the LiH crystal yield the core charge density spherical, like in the lithium atom: at the kinetic energy cutoff of 210 Ry, and with the density constructed from the core wave functions calculated at 10 special points $\vec{k}_i$, we find numerically that the maximum of the core radial density does not depend on the direction of $\vec{r}$ to within three decimals — whether $\vec{r}$ is chosen along a ''simple'' crystallographic direction such as [100], [110], or along an ''uneven'' one such as [17, 31, -17] or [36, 10, -11], which is not represented in the plane-wave expansion of the core density. The sphericity once checked out, it is interesting to compare the $1s$ core radial density calculated in the solid with the one calculated for the isolated lithium atom. This is done in Fig. 1, in which the two quantities are plotted, with the origin on the lithium atom. The figure demonstrates that the two densities

are, indeed, very close. They slightly differ in the position of the maxima — which is the ''radius'' of the core: 0.34 atomic units in the crystal versus 0.36 atomic units in the atom.

In order to further check whether this difference is not an artifact of the methods used, we have verified two other features of the maximum of the core radial density in the solid: it turns out that (1) the maximum does not depend on the lattice constant selected for the calculations in solid; (2) increasing the number of special points $\vec{k}_i$ used for the integration over the BZ from 10 to 28 does not shift the maximum of the core radial density.

Thus the small difference of 0.02 a.u. in the lithium core size is, apparently, an effect of a slight core polarization in the LiH crystal, as suggested, e.g., in Ref. 27. Also, the present calculations predict a core bandwidth of approximately 0.1 eV; the existence of the (weak) dispersion of this band evidences, as well, the same influence of the environment on the core wave functions. Before further discussing the calculations with the unscreened Coulomb potentials in Sec. V, we will now turn to the Compton effect.

IV. COMPTON PROFILES

A. The Compton effect

The Compton process is an inelastic scattering of a photon by an electron. The relationship between the double differential Compton cross section, which is the quantity measured experimentally, and the Compton profile (CP) is given (in atomic units, $\hbar=m=e=1$) by

$$\frac{d^2\sigma}{d\Omega\, d\omega_2}=\left(\frac{d\sigma}{d\Omega}\right)_{\mathrm{Th}}\frac{\omega_2}{\omega_1}\frac{J(\omega_1-\omega_2)}{|\vec{K}|}. \tag{5}$$

Here J is the CP, ω_1 and ω_2 are the energies of the incident and scattered photons, respectively, $(d\sigma/d\Omega)_{\mathrm{Th}}$ is the Thomson differential cross section and $\vec{K}$ is the scattering vector.

Within the impulse approximation (IA), adopting the independent particle and frozen orbital approximations, the CP can be expressed as (see Ref. 2)

$$J(q,\vec{e})=\int n(\vec{p})\,\delta(\vec{p}\cdot\vec{e}-q)\,d\vec{p}, \tag{6}$$

where $\vec{p}$ is the electron momentum in the initial state, $n(\vec{p})$ the momentum density of electrons, $\vec{e}$ the unit vector along $\vec{K}$, and q the projection of $\vec{p}$ along the scattering vector. We notice that the CP is a directional quantity (through the dependence on $\vec{e}$).

In typical experimental conditions (x-ray energy range), the IA is only valid for valence electrons and not for the core,[28] whereas the experiments measure a total CP that results from scattering on both groups of electrons. As the core-electron scattering is known not to be usually a ground-state property, an adequate treatment of the experimental data consists in subtracting from the measured CP the core contribution, calculated by using the quasi-self-consistent-field (QSCF) approximation[28–30] rather than the IA. Comparing then the experimental valence CP to the theoretical one obtained from Eq. (6) provides a direct test for the quality of the calculated ground-state valence-electron density.

Recently,[31] high-resolution x-ray measurements of Compton profiles have been performed on a LiH monocrystal for 12 different directions of the scattering vector. For three of them, two main corrections have been applied to the data,[11,32] viz., the contribution of the core electrons was evaluated using the QSCF approximation, and the effects of multiple scattering were taken into account (i.e., the possibility that one photon may scatter more than once in the sample). Neither of these two corrections turned out to be negligible.[11] Consequently, in the present paper we will use, for comparison with our theoretical results, these ''cleaned'' experimental data relating to the [100], [110], and [210] orientations of the scattering vector $\vec{K}$.

Both within the DFT and the Hartree-Fock approach, the ground-state charge density $n(\vec{r})$ in a nonmetallic solid can be written as a sum over one-electron wave functions $\psi_{n,\vec{k}}$ of the occupied states:

$$n(\vec{r})=\sum_{n,\vec{k}}|\psi_{n,\vec{k}}|^2. \tag{7}$$

$\vec{k}$ are the wave vectors restricted to the first Brillouin zone (BZ), and n runs over the bands.

With the plane-wave expansion of $\psi_{n,\vec{k}}$ [see Eq. (1)] and using Eq. (2), the *valence* Compton profile J of a nonmetallic crystal, in the IA, becomes[4]

$$J(q,\vec{e})=\frac{1}{N}\sum_{n}\sum_{\vec{k}}\sum_{\vec{G}}|C_{n,\vec{k}}(\vec{G})|^2\,\delta[(\vec{k}+\vec{G})\cdot\vec{e}-q]. \tag{8}$$

Here N is the normalization factor,[4] $\vec{G}$ stands for reciprocal-lattice vectors, and n is now limited to the valence states.

The Brillouin zone summation in Eq. (8) is carried out, in this work, using the tetrahedron method of Lehmann and Taut, and Jepsen and Andersen;[33] an irreducible segment of the Brillouin zone is divided into 33 tetrahedra having 22 common apices, and the $C_{n,\vec{k}}(\vec{G})$ coefficients are exactly calculated only on these 22 $\vec{k}$ points while a linear interpolation is performed inside each tetrahedron.

B. CALCULATIONS OF THE COMPTON PROFILES

In Fig. 2 two sets of theoretical valence Compton profiles are compared to the experimental ones, for the three directions already evoked in Sec. IV A. One set corresponds to the calculations with the unscreened Coulomb potentials and the other shows the results of pseudopotential calculations. The [100] Compton profile calculated from the reconstructed valence wave functions (and corresponding to the theoretical equilibrium predicted by the full Coulomb potential calculations) is also given in Fig. 2(a). A similar comparison for the anisotropies of CP is done in Fig. 3. The reconstruction procedure [see Eq. (4)] has been applied separately for every one of the 22 $\vec{k}$ points needed for the evaluation of the Compton profile from Eq. (8), and by choosing the atomic $1s$ orbital to describe the localized function of Eqs. (2) and (3). As a matter of fact, atomic calculations are the easiest source of information about the core orbitals; using them in solid nevertheless implies assuming tacitly the frozen-core

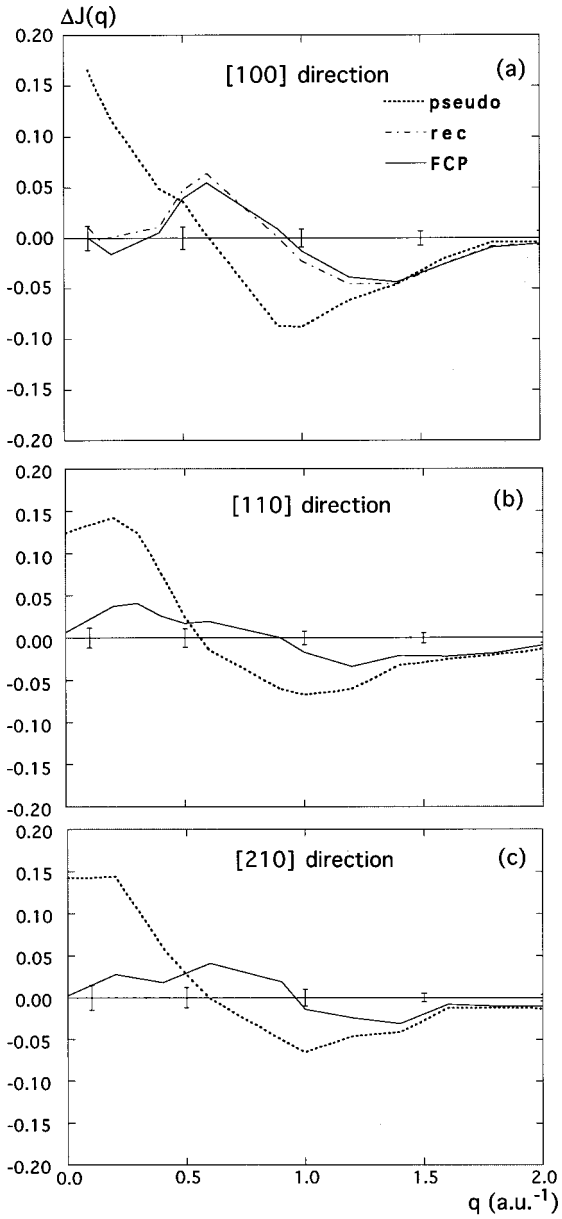

FIG. 2. Difference $\Delta J(q)$ between the theoretical and experimental valence Compton profiles corresponding to the [100] (a), [110] (b) and [210] (c) directions. The theoretical profiles have been evaluated with the full Coulomb potentials (cutoff of 210 Ry) or with pseudopotential (cutoff of 100 Ry), at the corresponding theoretical lattice constants. (a) also shows the result of the orthogonalization procedure starting from the pseudopotential calculations (cutoff of 100 Ry and with the lattice constant of the full Coulomb potential calculations, i.e., $a=3.91$ Å). All the theoretical Compton profiles have been convoluted with the experimental resolution (a Gauss function with the half-width of 0.19 a.u.). The experimental data were obtained as described in the Sec. IV. All profiles are normalized to 2 (the number of valence electrons per primitive cell); *pseudo* stands for the pseudopotential calculations, *rec* for the reconstruction procedure, and FCP for the full Coulomb potential ones. The error bars are the statistical error bars of the (experimental) data.

approximation. We have seen in Sec. III that the solid core density in LiH is indeed close to the 1*s* lithium atomic one, although Fig. 1 suggests that a slight polarization of the core may take place in the solid. The subsequent calculations can thus also be considered as a verification that the influence of the core polarization on the Compton effect is negligible in LiH.

We notice a marked disagreement of the theoretical CP's predicted by the pseudopotential approach with experiment: for example, at small values of q, the difference between theory and experiment is approximately 7 times larger than the experimental statistical error bars. On the other hand, it turns out that, due to compensation effects, the pseudopotential results for the anisotropies of the Compton profiles—i.e., results of subtraction between two different directional Compton profiles— agree with the experimental ones much better than the results on individual profiles. However, disagreements still remain: the results for the anisotropy displayed in Fig. 3(a) (which concerns the [100] and the [110] directions) and Fig. 3(b) (related to the [100] and the [210] directions) differ from the experiment at the values of q close to zero and, to some extent, for q around 0.8–1.0 a.u.

Unlike in the pseudopotential calculations, employing the full Coulomb potential yields both the theoretical profiles and anisotropies in very good agreement with the experimental ones; in particular, for the directional profiles, the discrepancies at the small q values have now disappeared and, with the exception of one point in Fig. 3(a), all values of the theoretical anisotropies are now within the experimental statistical uncertainties.

We can thus conclude that the behavior of the valence electrons in the lithium core region has an important effect on the valence Compton profiles. Obviously, this is a consequence of the fact that the valence-charge density obtained in the pseudopotential approach is not correct in the core regions. This incorrect description implies that the quantities deriving from the 1D or 2D integrals over charge density cannot be accurately reproduced in pseudopotentials calculations—unless the integrand is equal to zero everywhere in the core regions. On the other hand, due to the *norm-conservation* condition underlying the construction of the pseudopotential, the three-dimensional integrals over the pseudocharge density can be accurate, which would explain the success of the total energy pseudopotential method in the description of the basic static properties (Table I) and of similar quantities. Since the Compton effect implies integration of the electronic density in two dimensions [cf. the presence of δ function in Eq. (8)], it cannot be accurately calculated within the pseudopotential scheme for ionic systems, such as LiH, where a large part of the true valence density is around the nuclei. A simple orthogonalization procedure, which ''corrects'' the valence density around the nuclei, leads thus to very good results for the CP [see Figs. 2(a) and 3(a)]. We can see that the [100] Compton profile calculated using the orthogonalization scheme [Eq. (4)] is nearly identical with the one obtained with the unscreened Coulomb potential (and thus also with experimental results): the differences between the two theoretical results are much smaller than the experimental statistical error bars. The anisotropy of CP plotted in Fig. 3(a) demonstrates, as well, that the orthogonalization procedure makes it possible to reproduce, within the pseudopotential method, the result obtained with the full Coulomb potential. We have also checked for several other directions, and at several lattice parameters, that the

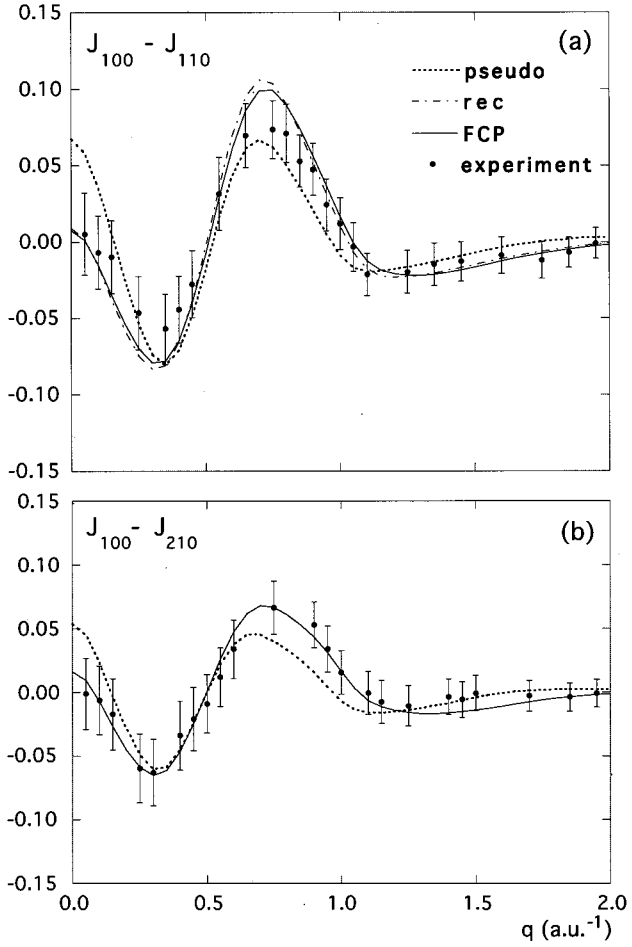

FIG. 3. Theoretical and experimental anisotropies of the Compton profiles corresponding to the differences [100]-[110] (a) and [100]-[210] (b). The theoretical profiles have been evaluated with the full Coulomb potentials (cutoff of 210 Ry) or with the pseudopotentials (cutoff of 100 Ry), at the corresponding theoretical lattice constants. (a) also shows the result of the orthogonalization procedure starting from the pseudopotential calculations (cutoff of 100 Ry and with the lattice constant of the full Coulomb potential calculations, i.e., $a=3.91$ Å). All the theoretical Compton profiles have been convoluted with the experimental resolution (a Gauss function with the half-width of 0.19 a.u.). The experimental data were obtained as described in the Sec. IV. All profiles are normalized to 2 (the number of valence electrons per primitive cell); *pseudo* stands for the pseudopotential calculations, *rec* for the reconstruction procedure, and FCP for the full Coulomb potential ones. The error bars are the statistical error bars of the (experimental) data.

present reconstruction method reproduces very well the valence Compton profile obtained in the full Coulomb potential calculations.

V. DISCUSSION

We performed LDA calculations, in a plane-wave basis, of the directional Compton profiles for LiH, and of their anisotropies. The results obtained with pseudopotentials are in rather poor agreement with experiment. The discrepancy between this type of calculation and measurements results from the impossibility for pseudopotentials to generate a realistic valence-charge density in the core region of lithium. We have demonstrated that by employing the full unscreened Coulomb potentials, i.e., by avoiding the pseudization of the wave functions, the theoretical Compton profiles and their anisotropies are in excellent agreement with experiment. One may then wonder if such an approach can be used for substances other than LiH.

To answer the question, we will now determine the cost of such a calculation which, obviously, is the cost of expressing by plane waves [see Eq. (1)] the core wave function $\psi_{1,\vec{k}}$ in any arbitrary crystal. Let us then take for the localized orbital of Eq. (2) the atomic $1s$ orbital of the heaviest atom in the crystal, and describe it by the hydrogenlike expression:

$$\phi_{\text{core}}(\vec{r})=\sqrt{\frac{\xi^3}{\pi}}\exp(-\xi r), \tag{9}$$

with ξ controlling the decay of the orbital. We then obtain from Eq. (3) for the coefficients of the plane-wave expansion at the Γ point:

$$C_{1,\vec{k}=\vec{0}}(\vec{G})\propto\frac{\xi^{2.5}}{(\vec{G}^2+\xi^2)^2}. \tag{10}$$

The proportionality coefficient can be easily expressed in terms of the $C_{1,\vec{k}=\vec{0}}(\vec{G}=\vec{0})$ — i.e., the spatial average of the wave function $\psi_{1,\vec{k}=\vec{0}}$ — so that finally

$$C_{1,\vec{k}=\vec{0}}(\vec{G})=C_{1,\vec{k}=\vec{0}}(\vec{G}=\vec{0})\frac{\xi^4}{(\vec{G}^2+\xi^2)^2}. \tag{11}$$

With the plane-wave cutoff energy, given in Ry, $E^{\text{pw}}(\text{Ry})$, the largest plane wave included in the expansion of the wave function at the Γ point corresponds to the wave vector $\vec{G}_{\max}$ given, in atomic units, by

$$E^{\text{pw}}(\text{Ry})=\vec{G}^2_{\max}(\text{a.u.}). \tag{12}$$

Let us introduce the ''convergence-error factor'' f_{ce} that expresses the ''quality'' of the convergence:

$$f_{\text{ce}}\equiv\frac{C_{1,\vec{k}=\vec{0}}(\vec{G}_{\max})}{C_{1,\vec{k}=\vec{0}}(\vec{G}=\vec{0})}=\frac{\xi^4}{[E^{\text{pw}}(\text{Ry})+\xi^2]^2}. \tag{13}$$

In this notation, the plane-wave expansion is cut off when the Fourier coefficients become f_{ce} times smaller than the average value of the wave function. Rewriting the above expression (13), the plane-wave cutoff required for obtaining a given convergence-error factor is

$$E^{\text{pw}}(\text{Ry})=\left(\sqrt{\frac{1}{f_{\text{ce}}}}-1\right)\xi^2. \tag{14}$$

One can estimate ξ by adopting the simple screening model of Slater; in terms of the effective charge and of the screening constant reflecting the presence of the other $1s$ electron, we get for any atom

$$\xi = Z - \sigma_{1s}, \tag{15}$$

where Z is the nuclear charge (of the heaviest atom in the crystal), $\sigma_{1s}=0.3$ for any atom heavier than hydrogen (see, e.g., Ref. 34) and $\sigma_{1s}=0$ for the hydrogen. We thus obtain

$$E^{\mathrm{pw}}(\mathrm{Ry}) = \left(\sqrt{\frac{1}{f_{\mathrm{ce}}}} - 1 \right) (Z - \sigma_{1s})^2. \tag{16}$$

According to this equation, the cutoff required to attain any given ''quality of convergence'' f_{ce} only depends on the heaviest atom present in the crystal and not at all on the crystal structure; this reflects the idea that the $1s$ electrons in a crystal are not sensitive to the environment. Also, we notice that Eq. (16) does not depend on the lattice constant — it is only the conversion of E^{pw} to the number of plane waves that does (both on the lattice constant and on the crystal structure). In our full potential calculations performed in the Sec. III B with the cutoff $E^{\mathrm{pw}} = 210$ Ry, the convergence-error factor [evaluated from its definition (13), and on the Fourier expansion actually used] reaches $f_{\mathrm{ce}} = 0.0009$. On the other hand, in terms of the Slater model, requiring $f_{\mathrm{ce}}=0.0009$ and $Z=3$, we find that the corresponding cutoff proposed by the Eq. (16) is approximately 235 Ry. This suggests the approximate uncertainty of the Slater model for E^{pw}: 10%.

For judging what the ''quality of convergence'' means in terms of the ''quality of the results,'' we have reported in Table II, the values of f_{ce} (evaluated, again, on the actual Fourier series) corresponding to the different E^{pw} used. They can be confronted with the quality of reproduction of the basic ground-state properties.

The above simple way of expressing the localized orbital and its exponential decay allows us to estimate, with rather good accuracy, the kinetic energy cutoffs required for achieving the convergence of the full Coulomb potential calculations in an arbitrary substance. Using Eq. (16), we can judge the feasibility of the plane-wave calculations with the full Coulomb potential for the next few elements of the Periodic Table: beryllium ($Z=4$), boron ($Z=5$), and carbon ($Z=6$). Choosing the same $f_{\mathrm{ce}}=0.001$ as in the present work, it turns out that the E^{pw} cutoff of approximately 400 Ry is needed for Be, 675 Ry for B, and 1000 Ry for C — which drastically limits the possibility of using the full unscreened Coulomb potential for compounds other than LiH; it is thus in the first row of the Periodic Table that we have to locate the border between the feasible and (presently) impracticable.

However, we have also shown that by starting from the more modest pseudopotential calculations and by using an orthogonalization method, it is possible to reproduce exactly the Compton profiles obtained in the full Coulomb potential calculations. This detour is numerically simple and computationally not costly, and it could be certainly generalized to larger systems composed of heavier atoms.

ACKNOWLEDGMENTS

The authors wish to thank B. Lévy, R.M. Martin, S. Rabii, and J. Ridard for valuable advice, Y. Garreau, J. Hutter, R.J. Needs, and M. Sauvage-Simkin for useful discussions, and G. Loupias for providing us with the experimental data of Ref. 31. The computer resources were provided by the Scientific Committee of IDRIS (Institut du Développement et des Ressources en Informatique Scientifique), Orsay, France.

*Present address : National Renewable Energy Laboratory, Golden, Colorado 80401.

[1] See, for example, *Compton scattering*, edited by B.G. Williams (McGraw-Hill, New York, 1977).
[2] P. Eisenberger and P.M. Platzman, Phys. Rev. A **2**, 415 (1970).
[3] See, for example, Z. Naturforsch. A, Phys. Phys. Chem. Kosmophys. (Germany) **48A** (1993).
[4] P. Rennert, Phys. Status Solidi B **105**, 567 (1981).
[5] R. Dovesi, C. Ermondi, E. Ferrero, C. Pisani, and C. Roetti, Phys. Rev. B **29**, 3591 (1984).
[6] R. Dovesi, C. Pisani, C. Roetti, and P. Dellarole, Phys. Rev. B **24**, 4170 (1981).
[7] M.Y. Chou, S.G. Louie, M.L. Cohen, and N.A.W. Holzwarth, Phys. Rev. B **30**, 1062 (1984).
[8] M.Y. Chou, M.L. Cohen, and S.G. Louie, Phys. Rev. B **33**, 6619 (1986).
[9] S. Rabii, J. Chomilier, and G. Loupias, Phys. Rev. B **40**, 10 105 (1989).
[10] G. Loupias, R. Wentzcovitch, L. Bellaiche, J. Moscovici, and S. Rabii, Phys. Rev. B **49**, 13 342 (1994).
[11] L. Bellaiche and B. Lévy, Phys. Rev. B **54**, 1575 (1996).
[12] J. Ihm, A. Zunger, and M. L. Cohen, J. Phys. C **12**, 4409 (1979).
[13] P. Hohenberg and W. Kohn, Phys. Rev. **136**, B864 (1964); W. Kohn and L.J. Sham, *ibid.* **140**, A1133 (1965).
[14] D.M. Ceperley and B.J. Alder, Phys. Rev. Lett. **45**, 566 (1980).
[15] J. Perdew and A. Zunger, Phys. Rev. B **23**, 5048 (1981).
[16] H.J. Monkhorst and J.D. Pack, Phys. Rev. B **13**, 5188 (1976).
[17] G.P. Kerker, J. Phys. C **13**, L189 (1980).
[18] S.G. Louie, S. Froyen, and M.L. Cohen, Phys. Rev. B **26**, 1738 (1982).
[19] F.D. Murnaghan, Proc. Natl. Acad. Sci. U.S.A. **50**, 697 (1944).
[20] J.L. Martins, Phys. Rev. B **41**, 7883 (1990).
[21] C.O. Rodriguez and K. Kunc, J. Phys. Condens. Matter **1**, 1601 (1989).
[22] J. Hama, K. Suito, and N. Kawakami, Phys. Rev. B **39**, 3351 (1989).
[23] K. Kunc, J. Chim. Phys. **86**, 647 (1989).
[24] V. Natoli, R.M. Martin, and D.M. Ceperley, Phys. Rev. Lett. **70**, 1952 (1993).
[25] R.M. Martin (private communication).
[26] M. Teter, Phys. Rev. B **48**, 5031 (1993).
[27] T. Asthalter and W. Weyrich, Z. Naturforsch. A, Phys. Phys. Chem. Kosmophys. (Germany) **48A**, No. 1-2, 303 (1993).
[28] A. Issolah, Y. Garreau, B. Lévy, and G. Loupias, Phys. Rev. B **44**, 11 029 (1991).
[29] A. Issolah, B. Lévy, A. Beswick, and G. Loupias, Phys. Rev. A **38**, 4509 (1988).
[30] A. Issolah, Y. Garreau, G. Loupias, and B. Lévy, Solid State Commun. **84**, 1099 (1992).
[31] J.M. Gillet, P. Becker, and G. Loupias, Acta Crystallogr. Sec. A **51**, 405 (1995).
[32] L. Bellaiche, J. Felsteiner, and G. Loupias (unpublished).

[33] G. Lehmann and M. Taut, Phys. Status Solidi B **87**, 221 (1978); O. Jepsen and O.K. Andersen, Solid State Commun. **9**, 1763 (1971).

[34] Y. Jean and F. Volatron, *Les Orbitales Moléculaires en Chimie. Introduction et Applications* (McGraw-Hill, Paris, 1991).

[35] G. Vidal-Valat, J.P. Vidal, K. Kurki-Suonio, and R. Kurki-Suonio, Acta Crystallogr. **48**, 46 (1992).

[36] D. R. Stephens and E. M. Lilley, J. Appl. Phys. **39**, 177 (1968).

[37] D. Gerlich and C. S. Smith, J. Phys. Chem. Solids **35**, 1587 (1974).